Novel Guests for Porous Columnar Thin Films: The Switchable Perchlorinated Trityl Radical Derivatives

ARTICLE *in* LANGMUIR · MARCH 2011

Impact Factor: 4.46 · DOI: 10.1021/la200470f · Source: PubMed

8 AUTHORS, INCLUDING:

Veronica Mugnaini
International Iberian Nanotechnology Labor…
44 PUBLICATIONS **937** CITATIONS
SEE PROFILE

Francisco Yubero
Spanish National Research Council
184 PUBLICATIONS **2,551** CITATIONS
SEE PROFILE

Jaume Veciana
Spanish National Research Council
983 PUBLICATIONS **12,373** CITATIONS
SEE PROFILE

Concepcio. Rovira
Spanish National Research Council
528 PUBLICATIONS **9,081** CITATIONS
SEE PROFILE

Langmuir

ARTICLE

pubs.acs.org/Langmuir

Novel Guests for Porous Columnar Thin Films: The Switchable Perchlorinated Trityl Radical Derivatives

Malena Oliveros,[†,§] Lola González-García,[‡,§] Veronica Mugnaini,[†] Francisco Yubero,[‡] Nans Roques,[†,∥] Jaume Veciana,[†] Agustin R. González-Elipe,[*,‡] and Concepció Rovira[*,†]

[†]Institut de Ciència de Materials de Barcelona (ICMAB-CSIC), Campus Universitari de la UAB, E-08193, Bellaterra, Spain;

[‡]Instituto de Ciencia de Materiales de Sevilla (CSIC-University of Sevilla), Avenida Américo Vespucio 49, E-41092, Sevilla, Spain

Supporting Information

ABSTRACT: TiO_2 and SiO_2 porous thin films consisting of tilted nanocolumns prepared by glancing angle evaporation (GLAD) have been infiltrated with guest derivatives belonging to the family of perchlorinated trityl radicals, novel guest molecules presenting an open shell electronic configuration associated with paramagnetism, fluorescence, and electroactivity. The main driving forces for infiltration from aqueous solutions of the carboxylate-substituted radical derivatives are the electrostatic interactions between their negative charge and the net positive charges induced on the film pores. Positive charges on the internal surface of the films were induced by either adjusting the radical solution pH at values lower than the point of zero charge (PZC) of the oxide or passivating the nanocolumns oxide surface with a positively charged aminosilane. The infiltrated composite thin films are robust and easy to handle thanks to the physical protection exerted by the film columns. They also keep the multifunctionality of the used guests, as confirmed by electron paramagnetic resonance (EPR), UV−vis spectroscopy, and fluorescence spectroscopy. To prove the electroactivity of the infiltrated porous films, a porous TiO_2 host layer was supported onto conductive indium tin oxide (ITO). By application of an appropriate redox potential, the guest radical molecules have been reversibly switched from their open-shell electronic configuration to their diamagnetic state and hence changed their optical properties. On the basis of these results, it is herein proposed that the appropriate surface functionalization of the pore internal surface of GLAD thin films can be used to prepare novel radical−oxide composite thin films usable for the development of robust switchable electrically driven photonic and magnetic devices.

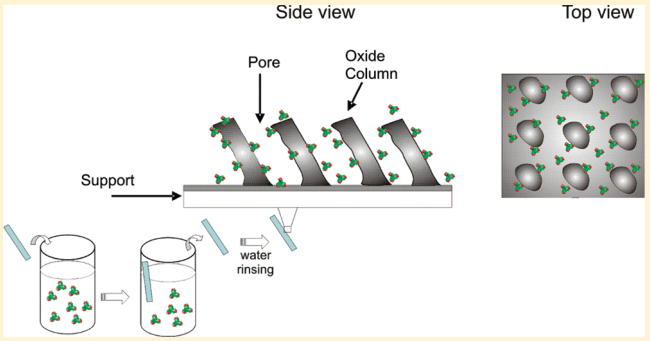

1. INTRODUCTION

Organic−inorganic hybrid materials have received considerable attention because they are a promising alternative to design new materials combining properties otherwise not achievable.[1] Perchlorinated organic trityl radicals (PTMs)[2] have been largely investigated thanks to their paramagnetism, electroactivity, as well as fluorescent properties.[3] They present a triphenylmethyl skeleton polysubstituted with chlorine atoms, the steric hindrance of which protects the central sp^2 carbon atom where most of the spin density resides, making them chemically and thermally stable. Interestingly, PTM radical derivatives present a rich electrochemical behavior since they can be easily and reversibly reduced to the anionic form or even oxidized to the cationic one, in both cases switching off their paramagnetic and fluorescent character.[4] The coexistence of so many different properties and the possibility to introduce on their skeleton functional substituents have made them unique synthons for the preparation of multidimensional and multifunctional materials.[3,5] In the latest years,[6] the possibility to functionalize gold,[7,8] graphite,[9] indium tin oxide (ITO),[10] or quartz[4] surfaces with perchlorinated radical derivatives, and hence transfer their properties to such solid supports, was explored toward the preparation of robust switchable devices. In these studies different approaches have been followed to anchor the PTM derivatives onto surfaces: covalent bonding, by means of substituted PTM radical derivatives that self-assemble on gold[7] or on passivated quartz;[4] noncovalent bonding, based on electrostatic interactions between a negatively charged carboxylate radical derivative and an oppositely charged anchoring layer;[4] and coordination bonding, by means of the use of a stepwise alternation of metal and organic layers.[11] Even if all these approaches have been successful, and robust paramagnetic and electroactive solid surfaces could be prepared, the so far obtained surfaces are not easily manageable since the adlayer is not physically protected. Moreover, on such planar surfaces the number of grafted molecules is proportional to the surface area. Since one of the requirements for the development of final devices is to handle a larger and controllable number of active

Received: February 4, 2011

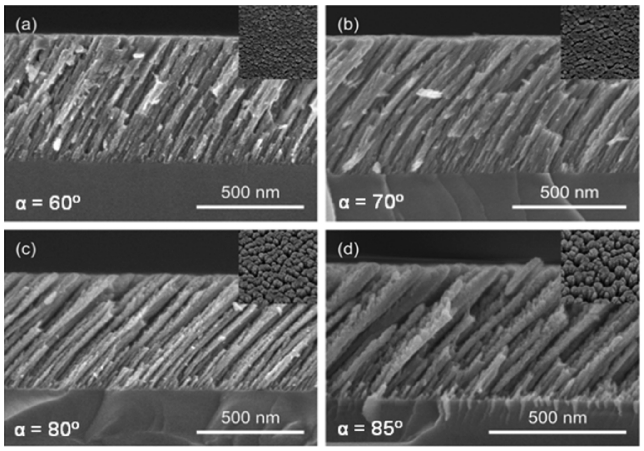

Figure 1. Cross-sectional and normal (inset) SEM micrographs of TiO_2 thin film prepared by GLAD at different glazing angles.

molecules, we have chosen as support inorganic oxide porous thin films obtained by glancing angle physical vapor deposition (GLAD).[12,13] GLAD oxide thin films are robust and transparent and have already been used to incorporate into their pores closed-shell fluorescent dye molecules and small metal particles with plasmon activity.[14] The obtained composite thin films were transparent and could be directly implemented into photonic devices. GLAD thin films and related structures have been used as photonic gas sensors[15] or wavelength shifters[16] or porous Bragg reflectors.[17] In the present work, we wanted to explore further the possibilities of this type of porous oxide thin films by incorporating in their structure radical derivatives with optical and magnetic properties that can be switched off by application of an appropriate voltage. For a successful incorporation of the carboxylic form of the radicals, we have developed several strategies of surface functionalization of the internal pore surface of the films to control the electrostatic interaction between the negatively charged radical derivatives and the positive charge induced by several functionalization strategies of the pore surface of the GLAD film. By the combination of different techniques, we have been able to demonstrate that after infiltration the radical is still paramagnetic and fluorescent. Moreover, by infiltration with such radical derivatives, the porous oxide films grown onto a thin conductive layer of ITO, we were able to demonstrate that optical properties of the guests can be electrochemically switched off in a reversible way, making these thin films manageable and robust redox switchable devices for different photonic applications. Furthermore, taking into account that the radical reduction is associated not only with a change in the optical properties but also with the loss of their paramagnetism, such hybrid thin films might open new possibilities for the fabrication of electrically activated magnetic devices, as well as mixed electrochromic and magnetic devices and photonic and magnetic sensors. In this paper we will describe the strategies used to infiltrate the PTM radical derivatives inside the empty spaces of transparent highly porous oxide thin films prepared by GLAD,[12,13] as well as the characterization of the obtained composite films. We demonstrate that the infiltrated hybrid organic−inorganic films of several hundreds of nanometers[12,13] can be used as manageable and robust redox switchable devices. Compared with previously investigated monolayer films of the PTM radical,[10] the films prepared in the present work permit one to incorporate a much larger amount of active

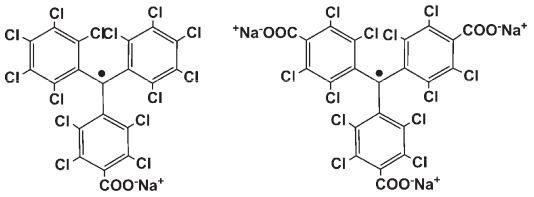

Figure 2. Chemical formulas of the sodium salts of the used radical derivatives.

molecules per unit area of the support while, simultaneously, providing an effective protection to the molecules embedded in the internal pores of the films.

2. EXPERIMENTAL SECTION

Preparation and Characterization of SiO_2 and TiO_2 Thin Films. Porous, transparent, and amorphous films of SiO_2 and TiO_2 to be used as host materials were prepared by GLAD at room temperature on quartz, quartz/ITO and silicon substrates. Evaporation was carried out in an electron bombardment evaporator by using TiO_2 and SiO_2 pellets as a target. Due to its geometry, films with a tilted columnar microstructure were prepared.[12,13] Different columnar thin films of SiO_2 and TiO_2 were obtained by performing the evaporation at glancing angles of 60°, 70°, 80°, or 85° in 10^{-4} Torrs of O_2. The typical thickness of the used films was 300 ± 30 nm. When using ITO as a support, 80 nm nanocolumnar TiO_2 films were deposited with an incident angle of 70° or 80°. A lower thickness was intended for these films to increase the efficiency in the redox switching experiments. To better appreciate the microstructure of the films by scanning electron microscopy (SEM) examination their thickness were on the order of 600 nm (Figure 1). The microstructure of the thin films deposited on a silicon wafer was examined by field emission scanning electron microscopy (FESEM) in a Hitachi S5200 microscope. Cross-sectional views were obtained by cleaving the silicon substrates.

It is apparent in the cross section views in Figure 1 that the film microstructure consists of tilted columns that leave free a great portion of the volume. All the GLAD thin films used as host in the present work show similar microstructures consisting of tilted nanocolumns extending from the interface with the substrate up to the external surface. The tilting angle of these columns and the porosity of the films increase in parallel to the evaporation angle.[12,13] The pore structure of these thin films consists of both micro- (according to the IUPAC, pores smaller than 2 nm) and meso- (pores higher than 2 nm) pores, most of them associated with the space between the columns. The total porosity ranges between 35% and 60% of the total film volume depending on the evaporation angle.[18] Due to their high porosity, a characteristic feature of these thin films is their low refractive index (n) with values ranging from approximately 1.7 to 1.5 for TiO_2 and from approximately 1.3 to 1.2 for SiO_2, for films prepared at the lowest and highest evaporation angles, respectively. These values were determined from the oscillations observed in the UV−vis absorption spectra.[19] UV−visible absorption/transmission spectra of the oxide films grown on quartz were recorded in transmission mode on a Cary 5000 UV−vis-NIR or on a Varian Cary 5 E spectrophotometer.

In general, we worked in transmission mode, which is the usual way of representing the spectra of thin films. It must be stressed that the thin films used for the infiltration experiments did not scatter the light and were transparent. This characteristic is critical if their implementation into photonic devices is an envisaged application.

Infiltration of the Radical Derivatives: Surface Functionalization of the Porous Films. The infiltration experiments were carried out with thin films of around 300 ± 30 nm thickness. The host

dx.doi.org/10.1021/la200470f |Langmuir XXXX, XXX, 000–000

Scheme 1. Scheme of the Infiltration Procedure[a]

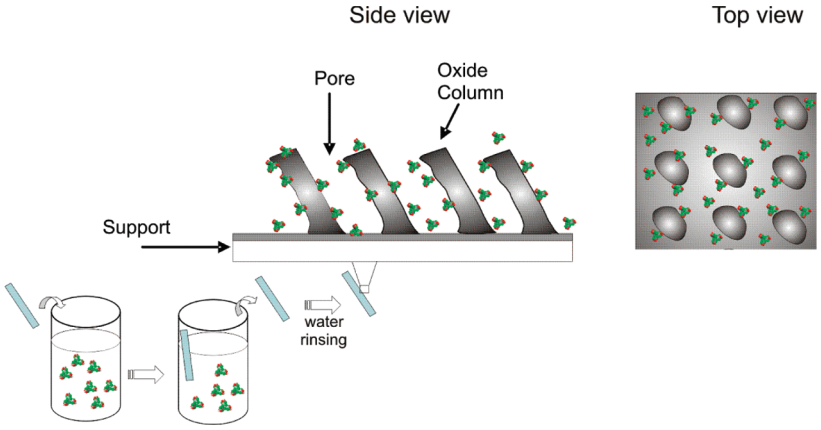

[a] On the bottom left part: A thin porous oxide film (in light blue) is immersed in an aqueous solution of the PTM derivative under study. After immersion the support is removed and rinsed with water.On the top part: side and top view of the nanostructure of the porous films. On the surface of the nanocolumns (gray), in between the pores, is located the PTM guest derivative **2Na$_3$**.

thin films have been infiltrated with the sodium salts of the mono- and/or tricarboxylic PTM derivatives (**1Na** and **2Na$_3$**) whose structure is reported in Figure 2. Both compounds have been synthesized as described previously.[20] For an efficient infiltration of the PTM derivatives, the internal surface of the films was functionalized by following two different strategies to promote their binding with the oxide films.

(A). Direct Binding. An (0.1−1 mM) aqueous solution of **2Na$_3$** was prepared at pH 2.3 that is lower than the point of zero charge (PZC) of TiO_2 (the PZC of TiO_2 is around 5.5[21]) and larger than the first pK_a value for this compound (see Supporting Information (SI)). This strategy aims to generate positively charged states on the internal surface of the TiO_2 to favor the electrostatic interactions between the surface and the negatively charged carboxylate (COO^-) functions. GLAD TiO_2 oxide films of different porosity were immersed into this solution for 2 h (Scheme 1) and then, the infiltrated films were abundantly rinsed with Milli-Q water to remove any radical molecule remaining unspecifically bound to the external surface of the films. Finally the films were dried under a soft nitrogen stream.

The low solubility of **1Na** in such an acidic medium (pH 2.3) made it impossible to incorporate it into the thin films by way of this approach.

(B). Indirect Binding. Nanocolumns of TiO_2 and SiO_2 films have been first covalently functionalized with *N*-[3-(trimethoxysilyl)-propyl]ethylenediamine by immersion of the films in a 5 mM distilled toluene solution of the silane under anaerobic conditions (argon atmosphere) for 4 h.[4] After abundantly rinsing with distilled toluene and drying with nitrogen, the films were introduced for a short time (5 min) in a *p*-toluene sulfonic acid aqueous solution at pH 4.5 in order to generate the NH_3^+ head of the silane. The positive charges of these groups are expected to interact with the negatively charged radical derivatives. The obtained modified thin films were then immersed for 2 h in the aqueous solution (0.1−1 mM) of either derivative **1Na** or **2Na$_3$** prepared with Milli-Q water and kept at their pH. The resulting infiltrated surfaces were rinsed with Milli-Q water and dried under a soft nitrogen stream.

Characterization of the Infiltrated Porous Films. When working with SiO_2 thin films, the absorbance signal of the radical $A(\lambda)$ (characteristic band at 380 nm) could be directly extracted from the experimental spectra after subtraction of the contribution of the host thin film, according to the following expression:

$$A(\lambda) = 1 - T(\lambda) \quad (1)$$

where $T(\lambda)$ is the normalized transmitted spectrum.

However, such a treatment was not feasible in the case of TiO_2 porous films because their transmittance spectra present an oscillatory behavior due to interference of the light at the substrate/film and film/air interfaces.[17] These oscillations are more pronounced with TiO_2 because of the relatively large differences between the n values of the film and those of the quartz substrate (i.e., around 1.4) and contribute to hide the absorption band characteristic of the infiltrated PTM radical derivatives. Moreover, since this oscillatory component is modified after the infiltration of the radicals, to get the signal of the infiltrated radicals it is not possible to proceed by subtracting the absorption spectrum of the bare TiO_2 from that of the composite radical/TiO_2 thin films. Therefore in this case the following expression is needed:

$$A(\lambda) = 1 - T(\lambda) - R(\lambda) \quad (2)$$

where $T(\lambda)$ and $R(\lambda)$ are the normalized transmittance and reflectance of the film-organic molecule system, respectively.

To extract the absorption band of the PTM radical derivatives, we have developed a mathematical procedure that permits one to approximate the absorbance spectra of the radicals in the films. We assume that the organic radical molecules are homogeneously distributed within the film matrix, so the effective refractive index $n(\lambda)$ of the radical-infiltrated film can be described by the Cauchy relationship:

$$n(\lambda) = n_0 + (n_2/\lambda)^2 \quad (3)$$

and the corresponding effective extinction coefficient $k(\lambda)$ by

$$k(\lambda) = k_0 + (k_1/\lambda) + c_{Eg}(\lambda_{Eg} - \lambda)^2 + G(\lambda) \quad (4)$$

where n_0, n_2, k_0, k_1, c_{Eg}, and λ_{Eg} are material parameters. The localized absorption of the radical derivatives is described with a Gaussian peak as

$$G(\lambda) = (A_g/\gamma_{radical}) \exp[-((w_{radical} - \lambda)/\gamma_{radical})^2] \quad (5)$$

with $A_{radical}$, $w_{radical}$, and $\gamma_{radical}$ are the intensity, position, and width of the localized absorption of the radical guest. Note that the previous description is only valid for weak absorption (i.e., $k(\lambda) \ll n(\lambda)$). In these conditions, an experimental transmitted spectrum can be simulated by a least-squared procedure, considering standard light transmission theory through a transparent or weakly absorbent film deposited on a transparent substrate.[19] The simulation of the transmitted spectra $T(\lambda)$ allows identifying the material parameters (n_0, n_2, k_0, k_1, c_{Eg}, l_{Eg}, $A_{radical}$, $w_{radical}$, $\gamma_{radical}$) that describe the characteristics of the radical-film system. The corresponding reflectance $R(\lambda)$ can be simulated as reported by Minkov.[22] Finally, the absorbance of the radical−film

dx.doi.org/10.1021/la200470f |*Langmuir* XXXX, XXX, 000–000

Scheme 2. Scheme of the two infiltration strategies used as explained in the text[a]

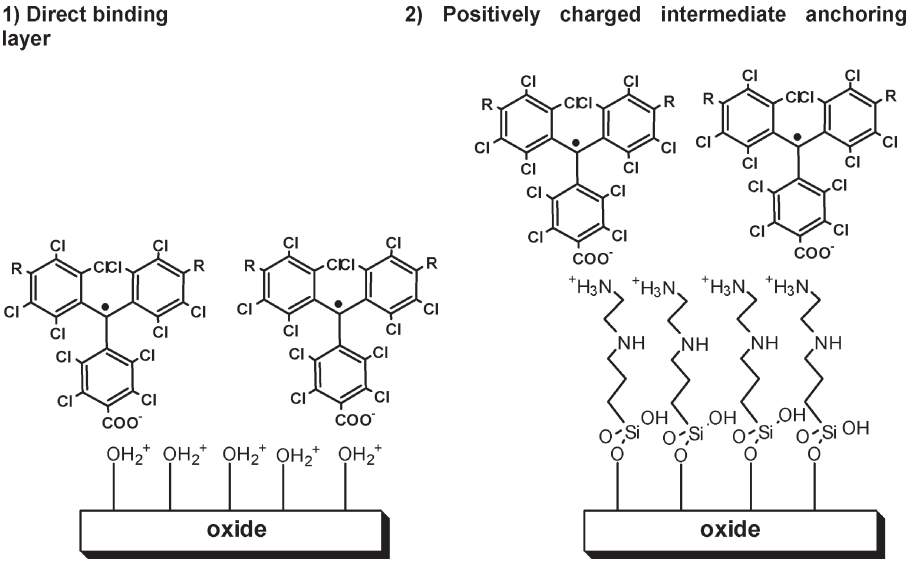

[a] For direct binding: R = COONa (**1Na**); oxide = TiO_2. For the use of an intermediate anchoring layer: R = Cl (**1Na**) or COONa ($\mathbf{2Na_3}$); oxide = TiO_2 or SiO_2.

system $A_{\text{radical-film}}(\lambda)$ is obtained using eq 2. The procedure assumes that the radical contribution to the absorption of the radical−film system is well reproduced by the Gaussian contribution to $k(\lambda)$. Thus, the absorbance spectra $A_{\text{radical}}(\lambda)$ corresponding only to the radical molecules incorporated into the film can be evaluated from the expression

$$A_{\text{radical}}(\lambda) = A_{\text{radical-film}}(\lambda) - A_{\text{film}}(\lambda) \quad (6)$$

where $A_{\text{film}}(\lambda) = A_{\text{film-radical}}$ is the simulated absorbance with $A_g = 0$. The specific results of this method are plotted in Figures SI1 and 5.

UV−vis spectroscopy has also been used to evaluate the amount of radical that can be incorporated (or released) from the film upon immersion of the infiltrated oxide films in water at an appropriate pH by following over time the decrease (or increase) in the absorbance at 385 nm of the aqueous solution at appropriate pH (lower and higher than PZC, respectively). These experiments have been performed by placing the quartz-supported titanium oxide thin film infiltrated with $\mathbf{2Na_3}$ on the lateral wall of a cuvette of 3.6 mL internal volume (see Figures S1 and S2 in the SI), so that the surface does not interfere with the absorption measurement.

The fluorescence in solution of derivatives **1Na** and $\mathbf{2Na_3}$ has been measured with a Perkin-Elmer LS45 equipped with a Hg lamp with slit apertures of 10 nm and a pass filter of 1%. When infiltrated in the porous surface, we used instead a Jobin-Yvon Fluorolog3 spectrofluorometer using grids of 2 nm for the excitation and emission.

Room-temperature electron paramagnetic resonance (EPR) spectra of all the infiltrated films have been recorded in a Bruker Elexsys spectrometer using an appropriate support for solid samples and a standard X-band cavity. The experimental parameters used to record the room-temperature spectra were the following: 4 scans; 19.77mW power; sampling time 40.96 ms; modulation amplitude 1.5G.

The time-of-flight secondary ion mass spectrometry (ToF-SIMS) analysis were performed on a ToF-SIMS-type ION-TOF IV instrument (IONTOF GmbH, Münster, Germany), equipped with a Bi polyatomic primary ion source, a Cs/electron impact dual source column (DSC), and a low-energy electron flood gun (for charge compensation of insulating samples). The incidence angle of both the Bi and Cs ion sources was 45°. The operating analysis conditions were as follows: sputter etching of the surface was accomplished with an electron impact O^{2+} ion beam of 2 keV (with a target current of 125 nA) rastered over a 300 μm × 300 μm area. A pulsed beam of 25 keV Bi ions, scanned over a 50 μm × 50 μm region centered within the sputtered area, was used to generate secondary ions for analysis in positive polarity. A high current beam of low energy (<20 eV) electrons was employed for charge compensation. Mass resolution ($m/\Delta m$) was higher than 6000, and full spectra from 1 to 800 amu were acquired during all the depths profiles.

The electrochemical experiments were performed with a potentiostat−galvanostat 263a from EG&G Princeton Applied Research, using as auxiliary electrode platinum wire and as a reference electrode a silver wire. The experiments were carried out in a 0.1 M solution of potassium chloride in acidic water (pH 2) to avoid desorption of the radical during the experiment and using the functionalized substrate as a working electrode (vs Ag(s)). In this approach we had to use a relatively thin (80 nm) TiO_2 film in order to have a better electrochemical signal, even though a lower thickness brought to a lower number of infiltrated radical molecules, and hence to a weaker UV−vis transmission.

3. RESULTS AND DISCUSSION

3.1. Strategies for PTM Radical Infiltration. The infiltration of the porous oxides in Figure 1 with guest molecules can be achieved by means of electrostatic interactions between the charged oxide internal surface of the pores and the oppositely charged guest molecule. By following this approach, positively charged rodhamine and porphyrin dyes have been successfully introduced inside the pores of negatively charged oxide host films.[14,16] In order to perform the infiltration of guest molecules with an open-shell electronic configuration, we have used the PTM radical derivatives **1Na** and $\mathbf{2Na_3}$ in Figure 2 with negatively charged carboxylate substituents that interact electrostatically with a positively charged thin film (Scheme 1). The functionalized thin films have been prepared as follows: (1) by working at a pH lower than the PZC, i.e., by direct binding (Scheme 2) or (2) by binding the negatively charged radical derivative with a positively charged silane anchoring layer, i.e., by indirect binding (Scheme 2).

Direct Binding Approach. To achieve the direct electrostatic binding of the PTM derivatives to the TiO_2 surface, the radical

dx.doi.org/10.1021/la200470f |*Langmuir* XXXX, XXX, 000–000

aqueous solution has been prepared at a pH (2.3−2.4 pH units) lower than the PZC of this oxide (PZC = 5.5), with the PZC[19] being the pH at which the charges of the oxide surface are balanced, to induce a net positive surface charge on its surface. Since at this low pH the **1Na** derivative was insoluble, this approach was used only for the infiltration of the $\mathbf{2Na_3}$ radical. As indicated by its pK_a values (pK_a1 = 1.2−1.4; pK_a2 = 2.8; pK_a3 = 6.9),[23] this latter derivative stays partially deprotonated at the working pH. Consequently, electrostatic interactions between the positively charged surface and the carboxylate ($-COO^-$) radical derivative should develop during the infiltration process. In order to remove any radical molecule unspecifically adsorbed inside the pores of the films, after the immersion of the film for 2 h inside the radical aqueous solution, the film was abundantly rinsed with water and then dried under gentle nitrogen stream. The so-prepared infiltrated films presented a reddish-yellowish chameleon-like coloration, suggesting that the reddish radical molecules were incorporated into the host thin film. The paramagnetic and optical properties of the radical-film surface were attested by means of EPR, UV−vis, and fluorescence spectroscopy. The EPR spectrum of a quartz-supported TiO_2 70° porous film after a 2 h immersion in a 0.1 mM aqueous solution (pH ∼2.3) of radical $\mathbf{2Na_3}$ (Figure 3) shows one single broad line (line width 6.3 G) centered at g = 2.0030(7), typical of a PTM radical derivative immobilized on a solid support,[4] indicating that the infiltration of the radical has taken place. The EPR technique allowed us to qualitatively investigate the effect of different immersion times on the signal intensity and hence address the efficiency of the infiltration and its dependence on the porosity of the oxide thin film. As shown in Figure 4 (on the right), when using a titanium oxide film with large pores (prepared at a glancing angle of 80°), the radical is fast incorporated inside the pores. Indeed, the difference in the signal/noise ratio when going from 30 to 65 min is quite high, whereas longer immersion times (from 65 to 120 min) do not significantly change the signal/noise ratio. By contrast, by using a less porous titanium oxide film (prepared at a glancing angle of 60°) (Figure 4, on the left) the rate of infiltration was slower and only after 120 min was the maximum intensity of the EPR signal reached. As the standard immersion time for all oxide films, independent of their porosity, we used 2 h as infiltration time.

Thanks to the characteristic absorption band of PTM derivatives, with a maximum at 380 nm, UV−vis spectroscopy has been useful to estimate the amount of infiltrated (or released) radical derivative molecules (as described in Figures SI2 and SI3). By following the decrease over time (2 h) in the UV−vis absorption spectrum of the radical solution (0.1 mM of derivative $\mathbf{2Na_3}$) at pH < PZC (pH 2.36) during infiltration in a TiO_2 70° GLAD film, it was possible to determine the total amount of infiltrated molecules (2.28×10^{16}, see Figure SI2), much higher than that expected for a flat surface. When using TiO_2 as the host film, the signal of the radical appeared superimposed to the oscillation characteristics of the bare thin film spectrum. To clearly observe the increase in the intensity of the band characteristic of the radical, the experimental spectra have been mathematically treated as described in the Experimental Section. As it can be seen in Figure 5, the experimental UV−vis transmission spectra of the infiltrated TiO_2 surface does not depict a feature that can be unambiguously attributed to the $\mathbf{2Na_3}$ radical. However, after the appropriate mathematical treatment described in the previous section, the absorbance spectrum could be directly assessed. The good agreement between the experimental and simulated transmission spectra clearly supports the consistency of the calculations. As it can be seen in Figure 5, the absorption signal of $\mathbf{2Na_3}$ increases with the immersion time and reaches saturation after 2 h, i.e., the maximum immersion period used in the experiments. Although the absorption spectra of the radical determined by calculation cannot be used for an exact description, neither of their shape nor their position, their intensities can be taken as representative of the actual concentration of the radical within the films. The absorbance spectra in Figure 5 clearly show that the amount of $\mathbf{2Na_3}$ radical increases with the immersion time and that the total amount at saturation is slightly higher for the 70° thin films. This result agrees with previous

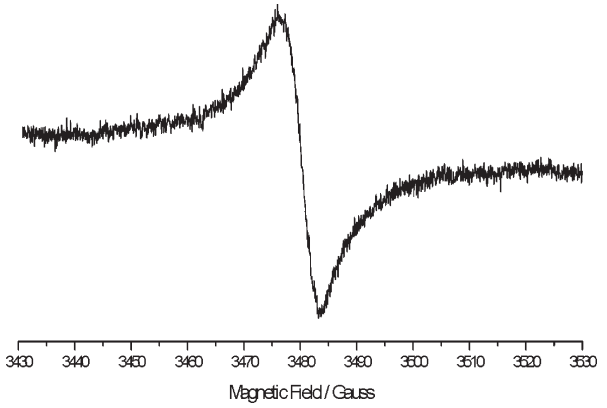

Figure 3. EPR spectrum of a quartz-supported TiO_2 70° porous surface after 2 h immersion in a 0.1 mM aqueous solution (pH 2.36) of radical $\mathbf{2Na_3}$. The measured g value is 2.0030(7), typical of these PTM derivatives.

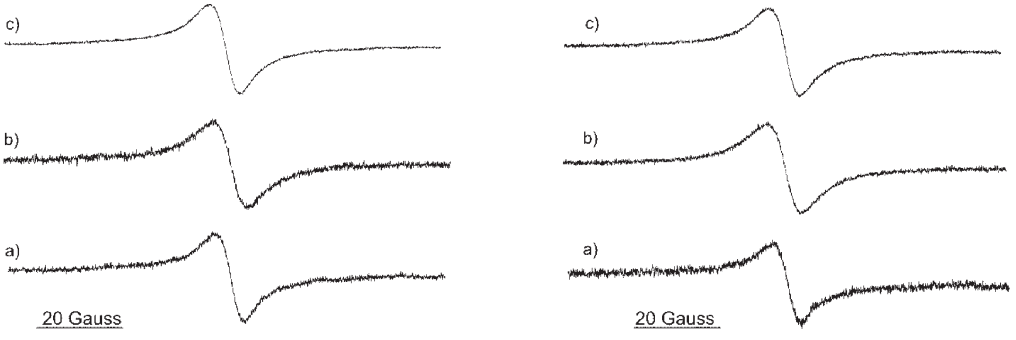

Figure 4. EPR spectrum of $\mathbf{2Na_3}/TiO_2$ composite thin films with different porosities and infiltration times ((a) 30 min; (b) 65 min; (c) 120 min). On the left: TiO_2 60°. On the right: TiO_2 80°. g values: 2.0030(5) and 2.0029(6) for 60° and 80° deposition angles, respectively.

dx.doi.org/10.1021/la200470f |*Langmuir* XXXX, XXX, 000–000

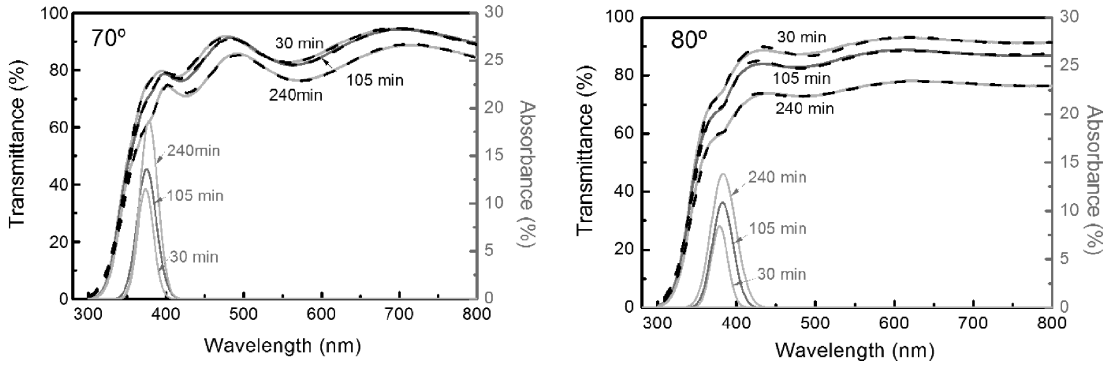

Figure 5. Experimental (solid gray line) and simulated (dotted black line) UV−vis transmission spectra recorded for **2Na$_3$**/TiO$_2$ composite thin films with different porosity (70° on the left and 80° on the right) and infiltration times (30 min; 105 min; 240 min). The mathematically extracted absorbance spectra of the radical are also plotted in the figure.

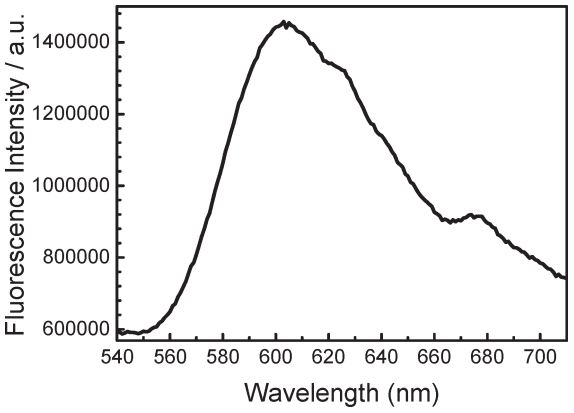

Figure 6. Fluorescence spectrum (λ_{exc} 380 nm) for a **2Na$_3$**/TiO$_2$ composite where the host thin films have been prepared by evaporation at 70°.

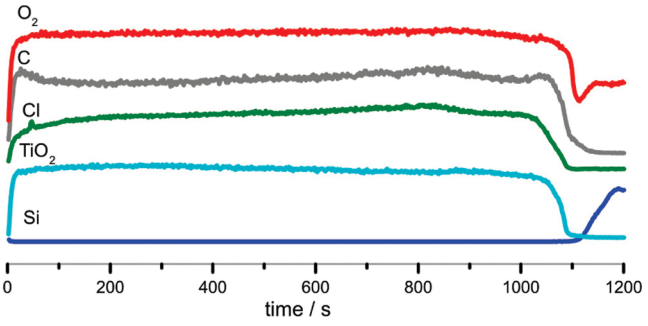

Figure 7. ToF-SIMS depth profile of a **2Na$_3$**/TiO$_2$ (80°) composite film showing the evolution of the masses: red, 32 (O_2); gray,12 (C); green, 35 (Cl); turquoise, 80 (TiO_2); and blue, 28 (Si).

evidence from literature in the sense that, for a given thickness, the 70° GLAD thin film presents a maximum surface area, even if it has a slightly lower pore volume.[24] Analogous results for the incorporation of **2Na$_3$** were obtained when using SiO_2 porous thin films (data not shown).

Fluorescence emission of PTM radical derivatives in general, and of **1Na** and **2Na$_3$** in particular, is a very important feature of these molecules and could be of interest for different photonic applications, mainly because of the large Stokes shift (>200 nm) that they present in solution (Figure SI4). Figure 6 presents the fluorescence spectrum, excited at λ = 380 nm, recorded for a **2Na$_3$**/TiO$_2$ composite with the host thin films prepared at a 70° evaporation angle when the maximum saturation of incorporated radicals is reached. The similar spectral shape in the films and in the aqueous solutions as well as the high intensity of the fluorescence spectra support the use of this type of thin films for photonic applications as switchable wavelength shifters.

Once we demonstrated that the paramagnetic and optical properties of these radical guests remain unaltered after infiltration, we addressed another crucial point, i.e., whether the incorporation of the radical molecules into the host thin films is homogeneous along the depth of the columns. ToF-SIMS depth profiles have been successfully used to check the extent of the infiltration,[25] i.e., to observe the depth of the guest penetration within the film. This advanced technique allows following the intensity of some detected ions over time, where the increase in time is correlated to the increase in depth. By following the change in the mass corresponding to TiO_2 (80 uam), we could determine the time at which we reached the oxide/quartz interface that corresponds to a sharp decrease in the mass of TiO_2 and a sharp increase in the mass of Si (i.e., Si fragments, uam 28), typical of the quartz support (Figure 7). At the same time we also observed that the intensity of the mass of the ions characteristics of the radical derivative **2Na$_3$** (carbon and chlorine, uam 12 and 35, respectively) is constant along the column length, but then abruptly decreases at the oxide/quartz interface. The loss in intensity of these masses at the interface and their parallel evolution with the characteristic mass of TiO_2 are clear demonstrations of a homogeneous distribution of the radical along the whole depth of the porous film.

Indirect Binding. By using this approach we could also study the incorporation of the radical derivative **1Na**, the low solubility of which at pH < PZC made impossible its incorporation into the oxide thin films by using the direct binding approach. In this case, the oxide surface (either SiO_2 or TiO_2) has been first covalently functionalized with an aminosilane (the trimethoxysilyl)-propyl]ethylenediamine, Scheme 2), then treated with an acid solution at pH 4.5 to generate the NH_3^+ head and eventually immersed in the aqueous solution of the radical derivatives **1Na** and **2Na$_3$** that bind via electrostatic interactions to the positively charged surface.[4] UV−vis (see Figure SI5) EPR, ToF-SIMS (see Figure SI6), and fluorescence spectroscopy gave evidence of the successful incorporation of both radical derivatives. As expected, the efficiency of the infiltration of radical derivatives **1Na** and **2Na$_3$** inside thin films with different porosities changed

dx.doi.org/10.1021/la200470f |*Langmuir* XXXX, XXX, 000–000

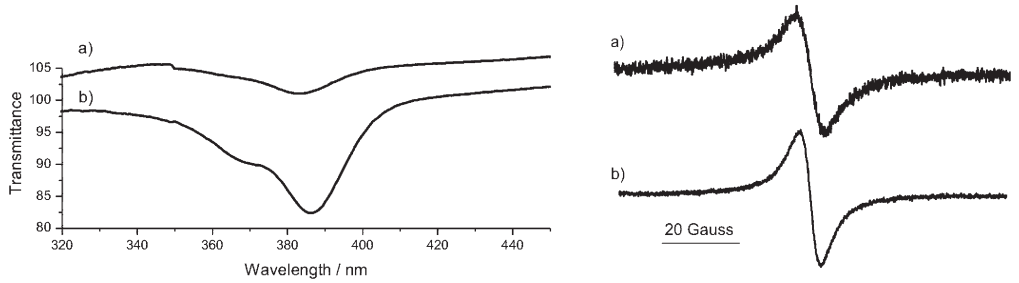

Figure 8. (Left) Transmittance UV−vis spectra and (right) EPR spectra of SiO_2 60° porous films functionalized with aminosilane and then infiltrated with $\mathbf{2Na_3}$ (a) and **1Na** (b). For EPR spectra: *g* values 2.0029(2) and 2.0034(6), respectively. Right: EPR spectrum.

Scheme 3. Scheme of the ITO Supported TiO_2 GLAD Evaporated Porous Thin Films[a]

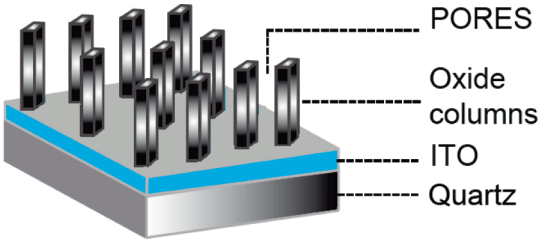

[a] For the sake of simplicity, the nanoculmns have been depicted orthogonal to the substrate rather than with the appropriate incident angle.

(Figure SI5, in the case of SiO_2) was higher for larger pores. Moreover, quite interestingly, both the UV−vis spectra (Figure 8A) and the EPR signals (Figure 8B) clearly indicate that the radical derivative **1Na** becomes more effectively incorporated within the film than the derivative $\mathbf{2Na_3}$. Although the reason for this result requires further analysis, we can suggest that the amount of incorporated radicals depends on both the electrostatic attraction between the carboxylate-substituted molecule and the positively charged surface and the electrostatic repulsion between nearby charged molecules. Taking this latter factor into account, the amount of $\mathbf{2Na_3}$ radicals would be smaller because of a higher intermolecular repulsion.

3.2. Electrochemical Properties of the PTM Radical-Oxide Films. PTM derivatives are electroactive species, the fluorescence and paramagnetism of which can be switched off by reduction or oxidation both in solution[3] and onto surfaces.[4] Particularly, the robust redox behavior of these derivatives when self-assembled onto the surface of ITO has been recently studied.[10] In order to check the redox behavior of PTM derivatives when incorporated by direct binding into the manageable porous oxide thin films, TiO_2 was evaporated by GLAD onto conductive ITO (supported on quartz) (Scheme 3) and used as a transparent working electrode for redox measurements. In order to favor the electrochemical reduction of the radical molecules residing along the nanocolumns, their height was kept to 80 nm. The obtained transparent host films, prepared by GLAD at incident angles of 70° or 80°, showed a final microstructure similar to the one prepared on inert quartz. Characteristic features of these films are a high porosity, a low refractive index, and the existence of long mesopores separating the oxide columns. When using ITO as a support for GLAD thin films with infiltrated radical derivatives (Scheme 3), it was possible to record the typical cyclic voltammogram (CV) of $\mathbf{2Na_3}$ infiltrated into TiO_2/ITO (Figure 9 (left)). The CV in water (pH 2) using KCl as the electrolyte recorded at a scan rate of 150 mV/s exhibits a reversible redox wave with an oxidation peak at 0.15 mV and a reduction peak at 0.094 mV. These peaks are characteristic of the redox processes converting the PTM radicals into the corresponding anions and vice versa.[7] We also observed that the peak current linearly increased with the scan rate, which is characteristic for surface-confined electroactive species (Figure 9, right).

To study the switching behavior, we applied alternatively the appropriate reductive (−0.05 V) and oxidative (0.3 V) potential, and the electroactive process was followed by UV−vis spectroscopy. In fact, while the PTM derivative $\mathbf{2Na_3}$ has a characteristic peak at 380 nm in its radical form, when the central carbon atom is reduced to the anion form, this band disappears, and a characteristic peak at 505 nm typical of the anion form develops in the spectrum. Since the oscillatory components of the TiO_2 transmission spectra preclude the direct observation of the band corresponding to the anion species, the redox process was followed by observing the disappearance in the radical band. By applying a reductive potential, we observed the loss of the band at 380 nm. By contrast, by applying an oxidative potential, the anion form was switched back to the radical form, and the appearance of the peak characteristic of the radical species at 380 nm was again observed. The electrochemical switching behavior could be reversibly observed over a long time period (40 min, Figure 10). This complete reversibility makes these hybrid films promising electrically switchable optical devices. Moreover, as expected from the known properties of this radical, its electrochemical reduction (directly observed by the loss of the absorption band at 380 nm) also leads to the removal of its paramagnetic character. Therefore, the hybrid radical−oxide porous films can be also considered as novel switchable redox magnetic devices.[26]

4. CONCLUSIONS

The experiments herein reported have demonstrated that the radical derivatives **1Na** and $\mathbf{2Na_3}$ can be successfully infiltrated into porous SiO_2 and/or TiO_2 thin films and that in the infiltrated state they retain all their properties (magnetic, optical, and electrochemical). The obtained thin films do not disperse the light, and by changing the film thickness as well as the porosity by selecting GLAD thin films prepared at different evaporation angles, as well as the infiltration conditions, it has been possible to control the amount of infiltrated radicals. For an efficient infiltration of the radical derivatives into the host films, their internal surface was functionalized by generating positively charged states that promote the electrostatic interactions with

dx.doi.org/10.1021/la200470f |*Langmuir* XXXX, XXX, 000–000

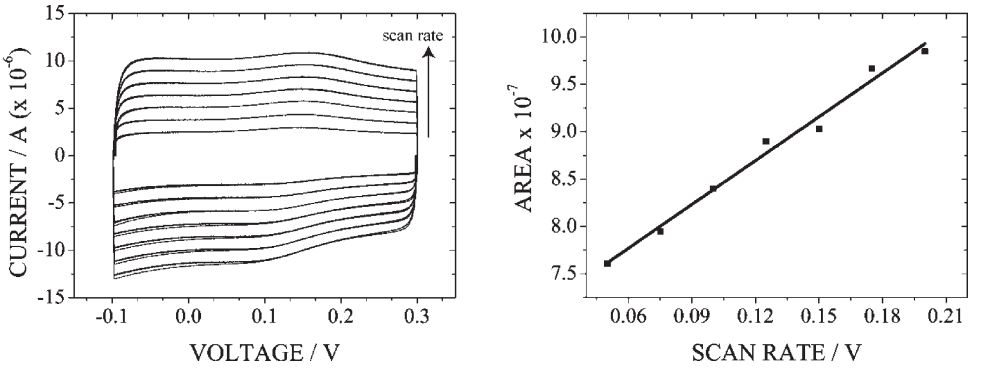

Figure 9. Left: CV of TiO_2 70° (80 nm) infiltrated with **2Na$_3$** at different scan rates (0.05, 0.075, 0.1, 0.125, 0.175, and 0.2 V/s). Right: Plot of the area of the CV at each scan rate versus the scan rate.

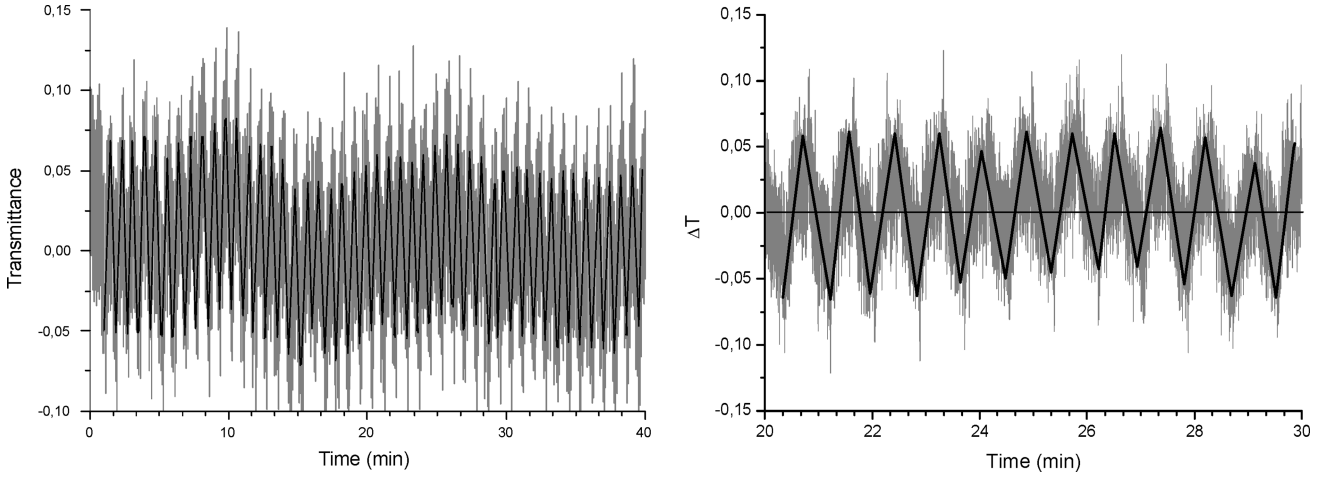

Figure 10. Redox switch of **2Na$_3$** on TiO_2 80° (80 nm). Left: The intensity of the band at 381 nm is followed over a time of 40 min applying a potential of −0.05 V for 25 s. Then the characteristic band is recovered by applying a potential of 0.3 V for 25 s. Right: Zoom of the time period 20−40 min corrected for the baseline.

the negatively charged carboxilate group of the radical derivatives. Control of pH during infiltration and direct binding to the nanocolumns surface or mediated by the anchoring of an appropriate aminosilane onto the oxide surface are the two selected functionalization strategies used to favor such electrostatic interaction.

In addition, it has been possible to fabricate easy to handle switchable thin films when they were supported on ITO conductive substrates. Using this type of substrate, both the optical (absorption and fluorescence) and the magnetic properties of the films can be reversibly modified by applying an external electrical voltage. The switching behavior, the easy handling, as well as the robustness of these radical-oxide composite thin films constitute essential conditions for the future development of robust electro-photonic/magnetic devices.

■ ASSOCIATED CONTENT

Supporting Information. Schemes and UV−vis spectra for adsorption and desorption of **2Na$_3$**; Transmittance UV−vis spectra of SiO_2 porous films infiltrated with **1Na**; SIMS depth profile of a **1Na**/TiO_2 (80°) composite film; methodology for determination of the pK_a of aqueous solutions of **2Na$_3$**. The material is available free of charge via the Internet at http://pubs.acs.org.

■ AUTHOR INFORMATION

Corresponding Author

*(C.R.) Fax: (+34) 93 580 5729; e-mail: cun@icmab.es. (A.R.G.-E.) Fax: (+34) 95 4460665; e-mail: arge@icmse.csic.es.

Present Addresses

[||]CNRS LCC (Laboratoire de Chimie de Coordination), 205 route de Narbonne, F-31077 Toulouse, France.

Author Contributions

[§]These two authors contributed equally to this experimental work.

■ ACKNOWLEDGMENT

This work was partially supported by the DGI Spain, (BIO2007-63458, CTQ2006-06333/BQU, CTQ2009-195011/BQU, CTQ 2010-19501/BQU, MAT 2007-65764, MAT2010-18447, MAT 2010-21228, Consolider CSD2008-00023, and LRB-ICTS), from the Generalitat de Catalunya, (2009SGR00516), the Junta de Andalucía (P09-TEP-5283), the Networking Research Center on

Bioengineering, Biomaterials, and NanoMedicine (CIBER-BBN), promoted by ISCIII, Spain, and by the EU Large Project One-P (FP7-NMP-2007-212311) and Marie Curie Est FuMaSSEC projects. V.M. acknowledges the MICINN-Spain for a Juan de la Cierva postdoctoral contract. The authors would like to thank Raul Perez from the Nanotechnology Platform of the Science Park of Barcelona for the TOF-SIMS measurements and analysis.

REFERENCES

(1) (a) Gómez-Romero, P., C. Sanchez, C. *Functional Hybrid Materials*; Wiley-VCH: Weinheim, Germany, 2004. (b) Kickelbick, G. *Hybrid Materials: Synthesis, Characterization, and Applications*; Wiley-VCH: Weinheim, Germany, 2007.

(2) Armet, O.; Veciana, J.; Rovira, C.; Riera, J.; Castañer, J.; Molins, E.; Rius, J.; Miravitlles, C.; Olivella, S.; Brichfeus, J. *J. Phys. Chem.* **1987**, *91*, 5608.

(3) (a) Veciana, J., Ratera, I. In *Stable Radicals: Fundamentals and Applied Aspects of Odd-Electron Compounds*; Hicks, R. G., Ed.; John Wiley & Sons, Ltd: New York, 2010; Chapter 2. (b) Mugnaini, V., Mas-Torrent, M., Ratera, I., Rovira, C., Veciana, J. In *Supramolecular Soft Matter: Applications in Materials and Organic Electronics*; Nakanishi, T., Ed.; John Wiley & Sons, Ltd: New York, in press (and references therein).

(4) Crivillers, C.; Mas-Torrent, M.; Perruchas, S.; Roques, N.; Vidal-Gancedo, J.; Veciana, J.; Rovira, V.; Basabe-Desmonts, L.; Jan Ravoo, B.; Crego-Calama, M.; Reinhoudt, D. N. *Angew. Chemie Int. Ed.* **2007**, *46*, 2215.

(5) Maspoch, D.; Ruiz-Molina, D.; Wurst, K.; Domingo, N.; Cavallini, M.; Biscarini, F.; Tejada, J.; Rovira, C.; Veciana, J. *Nature Mat.* **2003**, *2*, 190.

(6) Mas-Torrent, M.; Crivillers, N.; Mugnaini, V.; Ratera, I.; Rovira, C.; Veciana, J. *J. Mater. Chem.* **2009**, *19*, 1691.

(7) Crivillers, N.; Mas-Torrent, M.; Vidal-Gancedo, J.; Veciana, J.; Rovira, C. *J. Am. Chem. Soc.* **2008**, *130*, 5499.

(8) Mugnaini, V.; Fabrizioli, M.; Ratera, I.; Mannini, M.; Caneschi, A.; Gatteschi, D.; Manassen, Y.; Veciana, J. *Solid State Sci.* **2009**, *11*, 956.

(9) Crivillers, N.; Furukawa, S.; Minoia, A.; Ver Heyen, A.; Mas-Torrent, M.; Sporer, C.; Linares, M.; Volodin, A.; Van Haesendonck, C.; Van der Auweraer, M.; Lazzaroni, R.; De Feyter, S.; Veciana, J.; Rovira, C. *J. Am. Chem. Soc.* **2009**, *131*, 6246.

(10) Simão, C., Mas-Torrent, M., Crivillers, N., Lloveras, V., Veciana, J., Rovira, C., submitted.

(11) Shekhah, O.; Roques, N.; Mugnaini, V.; Munuera, C.; Ocal, C.; Veciana, J.; Wöll, C. *Langmuir* **2008**, *24*, 6640.

(12) Brett, M. J.; Hawkeye, M. M. *Science* **2008**, *319*, 1192.

(13) Hawkeye, M. M.; Brett, M. J. *J. Vac. Sci. Technol. A* **2007**, *25*, 5.

(14) Sánchez-Valencia, J. R.; Borrás, A.; Barranco, A.; Rico, V. J.; Espinós, J. P.; González-Elipe, A. R. *Langmuir* **2008**, *24*, 9460.

(15) (a) Rakow, N. A.; Suslick, K. S. *Nature* **2000**, *406*, 710. (b) Castillero, P.; Sánchez-Valencia, J. R; Cano, M.; Pedrosa, J. M.; Roales, J.; Barranco, A.; González-Elipe, A. R. *ACS Appl. Mater. Interfaces* **2010**, *2*, 712.

(16) Sánchez-Valencia, J. R..; Toudert, J.; González-Garca, L.; González-Elipe, A. R.; Barranco, A. *Chem. Commun.* **2010**, *46*, 4372.

(17) González-Garcia, L.; Lozano, G.; Barranco, A.; Míguez, H.; Gonzalez-Elipe, A. R. *J. Mater. Chem.* **2010**, *20*, 6408.

(18) Sánchez-Valencia, J. R..; Blaszczyk-Lezak, I.; Espinos, J. P.; Hamad, S.; González-Elipe, A. R.; Barranco, A. *Langmuir* **2009**, *25*, 9140.

(19) Minkov, D. A. *J. Phys. D: Appl. Phys.* **1989**, *22*, 1157.

(20) (a) Ballester, M.; Castañer, J.; Riera, J.; Ibàñez, A.; Pujades, J. *J. Org. Chem.* **1982**, *47*, 259. (b) Maspoch, D.; Domingo, N.; Ruiz-Molina, D.; Wurst, K.; Vaughan, G.; Tejada, J.; Rovira, C.; Veciana, J. *Angew. Chem. Int. Ed.* **2004**, *43*, 1828–1832.

(21) Kosmulski, M. *Chemical Properties of Material Surfaces*; Marcel Dekker: New York, 2001.

(22) Minkov, D. A. *J. Phys. D: Appl. Phys.* **1989**, *22*, 199.

(23) The pK_a of the derivative **2Na3** has been determined by potentiometric and spectrophtometric titration, as described in the SI. The three pK_a values referring to the deprotonation of the three carboxylic groups in a stepwise fashion are $pK_a1 < 1.2-1.4$, $pK_a2 = 2.8$, and $pK_a3 = 6.9$.

(24) Suzuki, M.; Taga, Y. *J. Appl. Phys.* **2001**, *90*, 5599.

(25) Wucher, A.; Cheng, J.; Zheng, L.; Winograd, N. *Anal. Bioanal. Chem.* **2009**, *393*, 1835.

(26) The electrochemical switch could not be monitored *in situ* by EPR since, when the surface was immersed in the polar electrolyte solution and submitted to the EPR microwaves, the molecules of PTM were desorbed from the surface, as clearly seen by the large narrowing of the signal line width.